# Directional Modulation Technique for Phased Arrays

Michael P. Daly, *Student Member, IEEE*, and Jennifer T. Bernhard, *Senior Member, IEEE*

***Abstract*—A directional modulation (DM) technique using a phased array to produce the modulation is presented. By phase shifting each element correctly, the desired amplitude and phase of each symbol in a digital modulation scheme can be produced in a given direction with data rates determined by the switching speed of the phase shifters. Because this signal is direction-dependent, the technique offers security, as the signal can be purposely distorted in other directions. DM also enables an array to send independent data in multiple directions. When using an array with driven elements, the phase shifts can be determined from simple calculations rather than time-consuming simulations or measurements. Mathematical analysis and experimental results are presented.**

***Index Terms*—Digital modulation, directional modulation, genetic algorithm, phase-shift keying (PSK), phased array.**

## I. Introduction

A PHASED array is advantageous for secure transmission because it reinforces the radiation pattern in the direction of the desired receiver while suppressing the pattern in most of the other directions. However, in conventional array transmission, the same information is still transmitted in undesired directions through sidelobes, and that information can be recovered with a sufficiently sensitive receiver. In an effort to lower sidelobes and provide more secure communication, past research has explored time-modulation in arrays. While conventional arrays have static element phase shifts and weighting, time-modulated arrays exploit an additional degree of freedom, time, in order to increase performance.

Research into time-modulated arrays has explored periodic switching of elements to mimic a static amplitude taper or a synthetic Doppler shift in order to achieve lower sidelobe levels [1]–[3]. More recent work has utilized differential evolution and genetic algorithms for pattern synthesis in time-modulated arrays [4], [5]. Instead of switching elements simply for radiation pattern synthesis, techniques have been proposed to synthesize a digital signal by switching array elements, along with the radiation pattern. These techniques can be used to deliver simple on-off keying [6], frequency shift keying [7], pulse-position modulation [8], or amplitude- and phase-based modulations [9], [10].

These schemes have the added benefit of directional-dependence. For instance, in [9], a continuous wave (CW) signal is modulated by an antenna composed of a single driven element with multiple switched parasitic elements. The driven element in this case was a dipole, and the states of many switches on the parasitic elements were set using a trial-and-error basis to actively change the amplitude and the phase of the signal in a desired direction, enabling distinct modulation constellation points that could be decoded by an intended receiver. At the same time, these switch configurations produce different signal characteristics in the undesired directions simply by virtue of the nature of the resulting antenna pattern. Since the constellation points in these undesired directions do not maintain their positions relative to each other, constellations can be created that are very difficult to demodulate in the presence of noise. In this way, the modulation is directional.

The parasitic array in [9] is not the only possible implementation of a directional modulation (DM) transmitter. Using an array with every element driven with the same CW signal, DM can be implemented by changing only the element weights. A diagram of a DM transmitter using phase shifters as the means of changing element weights is shown in Fig. 1, juxtaposed with a traditional phased array transmitter. The advantage of using an array of driven elements, as opposed to a parasitic array, is that the element weights necessary to synthesize a digital symbol can be found via simple calculation if the active element patterns are known. The active element patterns can be simulated or measured once and used for all subsequent calculations. On the other hand, it is not clear without a separate simulation or measurement how a certain combination of parasitics will change the radiation in a parasitic array. For this reason, a phased array with driven elements will be shown to be an effective and flexible DM transmitter.

For the very first time, a DM transmitter will be demonstrated using driven elements and an efficient algorithm for achieving digital modulations will be described. Furthermore, the security aspect of DM will be concretely measured using a bit error rate (BER) approach and multidirectional communication using DM will be demonstrated. A simple example illustrating the security aspect of DM is detailed in Section II. Next, Section III explains the mathematical background behind DM. Section IV gives the design steps to create a DM transmitter to send independent data in two different directions. Finally, Section V presents two examples illustrating the security aspect of DM.

## II. Directional Modulation Example

This example illustrates how the additional degrees of freedom of DM provide increased security. Consider a two-element array shown in Figs. 2 and 3 with an intended receiver ("Intended Rx") at broadside to the array and another undesired receiver ("Undesired Rx") at some direction. Fig. 2 is a block diagram of a traditional phased array transmitting, while Fig. 3

Manuscript received August 08, 2008; revised April 02, 2009. First published July 07, 2009; current version published September 02, 2009. The work of M. P. Daly was supported by an NDSEG Fellowship.

The authors are with the Electromagnetics Laboratory, Department of Electrical and Computer Engineering, University of Illinois at Urbana-Champaign, Urbana, IL 61801 USA (e-mail: jbernhar@illinois.edu).

Digital Object Identifier 10.1109/TAP.2009.2027047

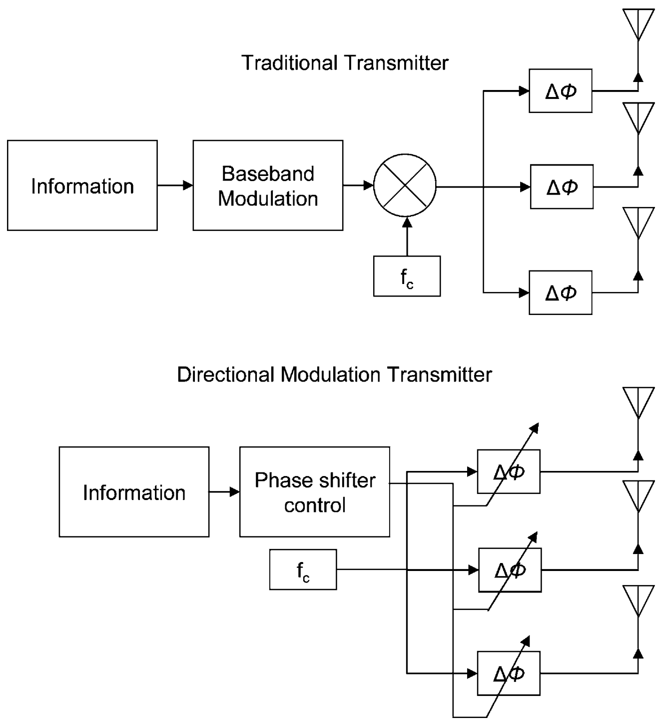


Fig. 1. Traditional array transmitter (top) and one implementation of a DM transmitter using phase shifters (bottom).

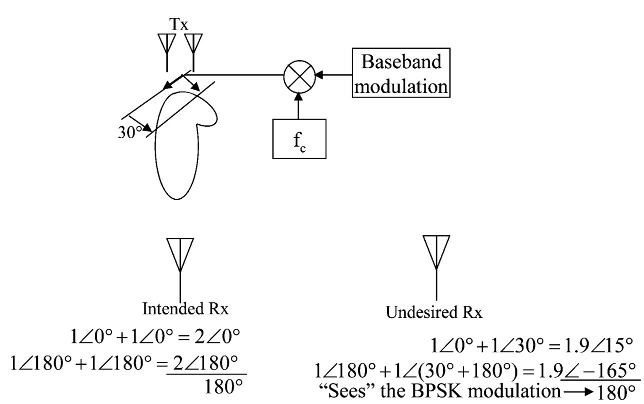


Fig. 2. Example of BPSK using a traditional array transmission scheme.

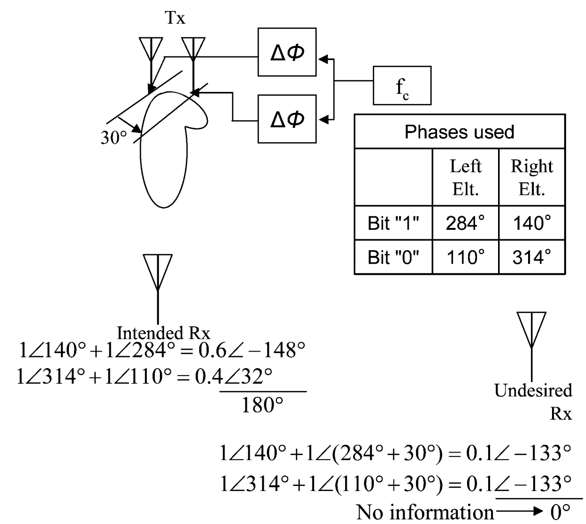


Fig. 3. Example of BPSK transmission using DM.

shows a phased array DM transmitter. Binary phase-shift keying (BPSK) modulation will be used by both transmitters.

In Figs. 2 and 3, there is 30° of extra path length at the carrier frequency from the left element to the undesired receiver relative to the right element. The simplified traditional means of sending BPSK is to multiply either a $+1$ or $-1$ with the carrier frequency. The baseband modulation block in Fig. 2 provides the $\pm 1$ and this is mixed with the carrier from the $f_c$ block in Fig. 2.

The voltage phasors representing the transmitted fields from each antenna are shown in Fig. 2 at both the intended and undesired receivers. The voltages are a function of the element radiation patterns, which for this example are assumed to be isotropic, and the relative phases introduced by the path from the transmitter to receiver.

In the traditional array case, the intended receiver sees $2\angle 0°$ when the transmitter sends a "1" and $2\angle 180°$ when the transmitter sends a "0". The undesired receiver also sees $1.9\angle 15°$ when the transmitter sends a "1" and $1.9\angle -165°$ when the transmitter sends a "0". The difference in amplitude at the undesired receiver owes to the extra 30° in path length from the left element relative to the right element. But these symbols still carry a 180° phase difference between a transmitted "1" and "0". If the undesired receiver can successfully demodulate the attenuated symbols, it can receive all of the same information that the intended receiver received.

The situation is different with DM presented in Fig. 3. The same two-element array is used, but this time there are two ideal phase shifters fed by the same carrier signal $f_c$. The phases are chosen so that the intended receiver sees a 180° phase difference when a "1" is sent versus a "0". In order to send a "1", the phase shifter for the left element is set to 284° and the phase shifter for the right element is set to 140°. To send a "0", the phase shifter for the left element is set to 110° and the phase shifter for the right element is set to 314°. When a "1" is sent, the intended receiver sees a voltage of $0.6\angle -148°$, while it sees a voltage of $0.4\angle 32°$ when a "0" is sent. Assuming the lower signal strength is still sufficient, the phase difference is still the desired 180° and thus the signal can be demodulated.

The undesired receiver in Fig. 3 sees something entirely different. When a "1" is sent, the undesired receiver sees $0.1\angle -133°$, while it receives $0.1\angle -133°$ when a "0" is sent. The undesired receiver receives no information. This is the essence of the security aspect of DM. A signal becomes distorted in both amplitude and phase off of the desired transmit direction. The distortion is a consequence of the fact that the modulation is produced by the array rather than at baseband. This distortion of both magnitude and phase does not occur in traditional array transmission.

The distortion caused by DM can also be understood from a channel-centric perspective. Traditionally, a signal is modulated in baseband and then upconverted to RF and passed through a fixed channel that includes phase shifters, antenna elements, and the propagation environment. DM, in contrast, passes a fixed signal through the channel and it is the channel that is actually modulated. In this case, the phase shifters provide the modulation, but the antenna elements could have provided the modulation such as in [9], [10]. When phase shifters are changed, the channel transfer function changes differently for different directions. This allows a DM signal to be distorted in undesired directions or to send multiple independent signals simultaneously.

An undesired receiver also could have been denied any information if a null were steered in its direction. Methods of null steering for arrays are well-known [11], [12]. But if the location of the desired receiver is not known, it is impossible for an array to steer nulls in every undesired transmit direction because of the presence of sidelobes. It will be shown in Section V that DM can create distortion in almost every undesired transmit direction even if sidelobes exist, and this method prevents eavesdropping even without knowledge of the location of undesired receivers.

## III. Phased Array Theory

In this section, we assemble basic beamforming equations in a format that allows direct use by genetic algorithms. This formulation also helps provide a clear linkage between radiation pattern synthesis and digital symbol synthesis. From [13], we can express the radiation pattern of an arbitrarily-spaced three-dimensional array of $N$ elements as

$$E(\theta,\phi)=\sum_{n=1}^{N} f_n(\theta,\phi)e^{j\mathbf{k}\cdot\mathbf{r}_n} \tag{1}$$

where $f_n(\theta,\phi)$ is the active element pattern of element $n$, and

$$\mathbf{k}\cdot\mathbf{r}_n=\frac{2\pi}{\lambda}(x_n\sin(\theta)\cos(\phi) +y_n\sin(\theta)\sin(\phi)+z_n\cos(\theta)) \tag{2}$$

$(x_n,y_n,z_n)$ is the location of element $n$ and $\lambda$ is the wavelength at the carrier frequency. The radiation pattern in (1) can be made time-varying by adding excitations $s_n(t)$ to each element

$$E(t,\theta,\phi)=\sum_{n=1}^{N} f_n(\theta,\phi)e^{j\mathbf{k}\cdot\mathbf{r}_n}s_n(t). \tag{3}$$

For a specific time $t$ and direction $(\theta,\phi), E(t,\theta,\phi)$ is a complex digital symbol with a magnitude and a phase that can be viewed as a constellation point on the real-imaginary coordinate system. If line-of-sight (LOS) communication is used and the array transmits in $K$ directions, then for each symbol period, $K$ symbols are synthesized simultaneously. Equation (4) shows how the excitations can be found to produce these $K$ symbols at time $t$. Equation (4), at the bottom of the page, is solved by matrix inversion to find the element excitations to produce a set of symbols. This assumes the magnitudes of the weights may vary. In the phased array considered in this present work, only the phase may vary and the magnitudes must be unity. Hence, an algorithm must be used to optimize the weights since they can no longer be solved directly because of this constraint. Section IV.B gives a genetic algorithm used to solve for communication simultaneously in two directions.

It is important to note that (4) only takes into account the goal of transmitting $K$ independent signals in $K$ directions, and neglects purposely distorting the signal everywhere else. The signal will be automatically distorted by virtue of its direction-dependence, but there is no way with (4) alone to specify the amount of distortion in each direction. Section V.A discusses how element weights can be found that purposely distort the signal in all undesired transmit directions.

Finally, all examples in this work assume LOS communication between the transmitter and each receiver. For non-line-of-sight communication, the array matrix in (4) can be replaced with a channel matrix, and the product gives digital symbols at locations instead of directions. Let $S(\bar{r}_n)$ be the complex symbol at location $\bar{r}_n$. Let $h_n(\bar{r})$ be the channel tap from element $n$ to the receiver at $\bar{r}$. The channel tap is a summation of all paths between element $n$ and the receiver at $\bar{r}$. The same analysis can now be conducted in a multipath environment, using the following equation

$$\begin{bmatrix} S_{\bar{r}_1}(t)\\ \vdots\\ S_{\bar{r}_K}(t)\end{bmatrix}=\begin{bmatrix} h_1(\bar{r}_1) & \cdots & h_N(\bar{r}_1)\\ \vdots & \ddots & \vdots\\ h_1(\bar{r}_K) & \cdots & h_N(\bar{r}_K)\end{bmatrix}\begin{bmatrix} s_1(t)\\ \vdots\\ s_N(t)\end{bmatrix}. \tag{5}$$

If the time-separation of the multipath is longer than the symbol time (so there is intersymbol interference) then a more complicated analysis than (5) is required.

The next two sections detail procedures for finding the element weights in (4) to make possible multidirectional and secure communication using only phase shifters in the transmit array.

## IV. Multidirectional Communication

In this section, measured active element patterns of a four-element array are used to demonstrate independent QPSK transmissions toward a receiver at $-30°$ from broadside and one at $+30°$ from broadside. Just as with the DM transmitter in Fig. 1,

$$\begin{bmatrix} E(t,\theta_1,\phi_1)\\ \vdots\\ E(t,\theta_K,\phi_K)\end{bmatrix}=\begin{bmatrix} f_1(\theta_1,\phi_1)e^{j\mathbf{k}\cdot\mathbf{r}_1} & \cdots & f_N(\theta_1,\phi_1)e^{j\mathbf{k}\cdot\mathbf{r}_N}\\ \vdots & \ddots & \vdots\\ f_1(\theta_K,\phi_K)e^{j\mathbf{k}\cdot\mathbf{r}_1} & \cdots & f_N(\theta_K,\phi_K)e^{j\mathbf{k}\cdot\mathbf{r}_N}\end{bmatrix}\begin{bmatrix} s_1(t)\\ \vdots\\ s_N(t)\end{bmatrix}. \tag{4}$$

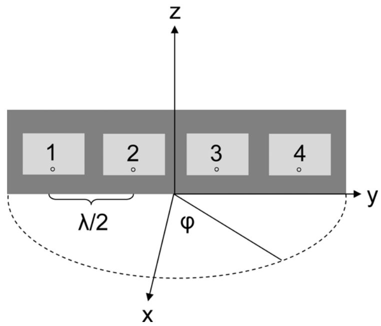


Fig. 4. Four-element linear patch array transmitting at 7 GHz.

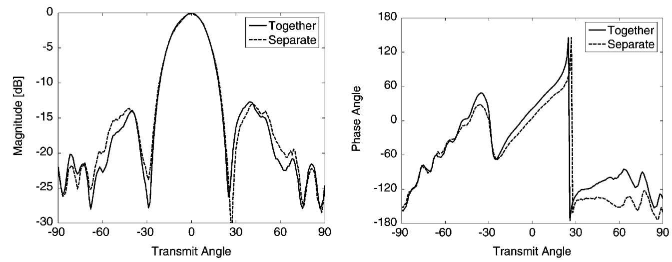


Fig. 5. Normalized magnitude and phase of the measured radiation pattern when all elements are driven (together) and the pattern predicted by the summation of the active element patterns (separate).

a CW signal is fed into each element and the modulation is implemented by phase shifters. Simulated radiation patterns and modulations from the measured element pattern data are generated, assuming lossless, continuous phase shifters. The measurement of the active element patterns is explained first, followed by an explanation of the genetic algorithm used to find suitable sets of phase shifts, and finally, the calculated results.

### A. Active Element Patterns

The active element pattern (or scan element pattern) is the radiation pattern of a single element when it is located in an array [14], [15]. It is different than the isolated element pattern due to mutual coupling between array elements and surface wave loss, and it is necessary to include these effects so that digital modulation magnitudes and phases are precise.

The antenna array to be measured for all calculations in this paper is a four-element linear array of microstrip patches, shown in Fig. 4. The operating frequency is 7 GHz, and all elements are spaced one-half of a wavelength apart. At the operating frequency, the return loss of all elements is greater than 12 dB. All patterns are taken in the azimuthal plane $(xy)$ and E-plane $(\hat{z})$ polarization is used with the plane of the array in the $yz$ plane.

The active element pattern of each element in the array is measured with all other elements terminated in 50 Ω. Because Maxwell's equations are linear, the total radiation pattern of the array is the superposition of the active element patterns [13]. This is confirmed in Fig. 5, in which the radiation pattern when all elements are uniformly driven is compared to the summation of the four active element patterns, for azimuthal angles $(\phi)$ from $-90^\circ$ to $+90^\circ$ corresponding to the half plane in front of the array. As expected, there is good agreement meaning that the active element patterns can be used for precise calculations.

### B. Optimization for Specific Symbols

An efficient optimization algorithm for DM to determine the phase shifts necessary to implement a digital modulation is presented. A genetic algorithm (GA) was chosen for this application because GAs have been used numerous times for array pattern synthesis, including nulling [12] and sidelobe reduction [16], [17]. In the scenario chosen, we are communicating in two different directions using a modulation with four symbols (QPSK), thus sixteen different sets of phase shifts must be generated. Each of these sixteen pairs of symbols can be found through the same optimization procedure.

The GA attempts to minimize a cost function that is the sum of the square magnitudes between the desired constellation points and the transmitted points on a constellation diagram. Assume there are $K$ desired constellation points (at $K$ different transmit directions). The desired modulation symbol in the $i$th direction is given by $E_{\text{desired}}(\theta_i, \phi_i)$ and the calculated modulation symbol from the current set of phase shifts is given by $E_{\text{calculated}}(\theta_i, \phi_i)$. The cost function is defined as

$$F = \sum_{i=1}^{K} |E_{\text{desired}}(\theta_i, \phi_i) - E_{\text{calculated}}(\theta_i, \phi_i)|^2. \quad (6)$$

We will denote the variables to be optimized (the phase shifts) as $\gamma_i$ for the $i$th element. The excitations are forced have magnitude equal to one by

$$s_i(t) = \exp(j\gamma_i(t)). \quad (7)$$

Members of the population are sets of four phase angles $\gamma$, one for each element. The population size was set to four, with children formed from random crossover of the two best members.

### C. Calculated Results

The resulting digital symbols and radiation patterns from the output of the GA are shown next. For the sake for brevity, only four of the sixteen possible pairs of symbols of these will be shown in Table I and Figs. 6 and 7. The desired constellation points, along with the phase shifts that produce them, are specified in Table I by their angle, i.e., 45° refers to the constellation point in the upper right quadrant.

As evident in Fig. 6, the GA does well at finding phase shifts that produce the desired phases while keeping all amplitudes approximately the same, as all constellation points are approximately the same distance from the origin. Fig. 7 shows the radiation patterns for each of the four phase combinations in Table I. Note that the radiation patterns of the array configured to send symbols in these two directions do not necessarily result in traditional beamforming in these directions.

## V. Directional Modulation For Security

Although DM provides inherent distortion in a signal as a function of direction, it is more desirable from a security aspect

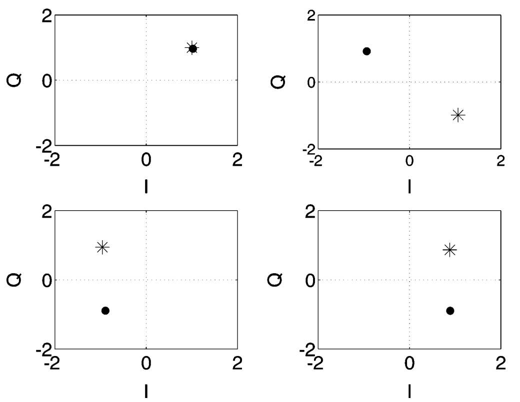


Fig. 6. Calculated QPSK constellation points at $-30°$ (circle) and $+30°$ (star) from broadside.

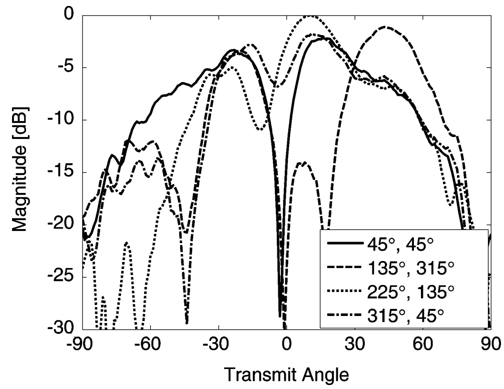


Fig. 7. Normalized radiation patterns when phased to create the symbols shown in Fig. 6.

TABLE I
PHASE SHIFTS TO PRODUCE QPSK SYMBOLS SIMULTANEOUSLY IN TWO DIRECTIONS

| **Desired symbols** | | **Required phase shift** | | | |
|---|---|---|---|---|---|
| **Dir. $-30°$** | **Dir. $+30°$** | **Elt. 1** | **Elt. 2** | **Elt. 3** | **Elt. 4** |
| $45°$ | $45°$ | $20°$ | $87°$ | $-84°$ | $-144°$ |
| $135°$ | $315°$ | $123°$ | $-62°$ | $-159°$ | $15°$ |
| $225°$ | $135°$ | $-17°$ | $111°$ | $-12°$ | $88°$ |
| $315°$ | $45°$ | $-15°$ | $25°$ | $-28°$ | $-166°$ |

to be able to maximize or minimize the BER in each direction. As a top layer of security, ideally all desired receivers should demodulate a signal with no bit errors while all eavesdroppers should demodulate a signal with as many bit errors as possible. Section V.A explains the necessary changes to the GA and how the resulting BERs were calculated. Then Sections V.B and V.C give two examples when the desired receiver is at transmit array broadside and $-45°$ away from broadside.

### A. *Optimization for BER*

The only change necessary to the GA from Section IV.B involves the cost function. Let $L$ be the set of directions in which low BER is desired, $H$ be the set of directions in which high BER is desired, $w_i$ and $w_j$ be weights chosen based on the importance of the BER in certain directions, and $(\theta_i, \phi_i)$ and $(\theta_j, \phi_j)$ represent transmit directions. Instead of (6), a new cost function is given as follows:

$$F = \sum_{i \in L} w_i \cdot \mathrm{BER}(\theta_i, \phi_i) - \sum_{j \in H} w_j \cdot \mathrm{BER}(\theta_j, \phi_j). \quad (8)$$

The BER is a function of the noise power (assumed to be equal in all directions) and the received constellation, assuming both the desired receivers and eavesdroppers have perfect knowledge of the channel and thus also knowledge of the received constellation diagrams.

How BER is calculated is described next. DM creates arbitrary four-point (4-ary) constellations rather than square QPSK constellations. Because the BERs of these constellations must be repeatedly calculated as part of the GA, it is desirable to have a closed-form expression of BER. While methods have been found to determine closed-form expressions for arbitrary constellations [18]–[20], these methods are complicated and instead a simple bound similar to the nearest-neighbor approximation [21] is used. The nearest-neighbor approximation states that the probability of symbol error can be approximated by the distance of the two closest constellation points

$$P_{\text{error}} = Q\left(\frac{d/2}{\sqrt{N_0/2}}\right) \quad (9)$$

where $d$ is the Euclidean distance between the two closest constellation points, $N_0/2$ is the noise power spectral density, and $Q(x)$ is the complementary Gaussian error function. This assumes that there is only one closest point or one nearest neighbor to each point, which is a valid assumption for the 4-ary constellations considered here. Next, the bound can be made more precise by considering the probability of symbol error of each constellation point separately. Let $d_i$ be the minimum Euclidean distance from point $i$ to any other constellation point. Then, assuming all four constellation points are equally likely, the probability of symbol error is given by

$$P_{\text{error}} = \frac{1}{4} \sum_{i=1}^{4} Q\left(\frac{d_i/2}{\sqrt{N_0/2}}\right). \quad (10)$$

Finally, by Gray coding, we can approximate the probability of bit error as half the probability of symbol error for a 4-ary constellation [21]. The final expression for a lower bound on BER is given by

$$P_b(\text{error}) = \frac{1}{8} \sum_{i=1}^{4} Q\left(\frac{d_i/2}{\sqrt{N_0/2}}\right). \quad (11)$$

This expression was used in the GA to evaluate the cost function in (8). It will be shown in Sections V.B and V.C that this bound closely predicts the simulated BERs.

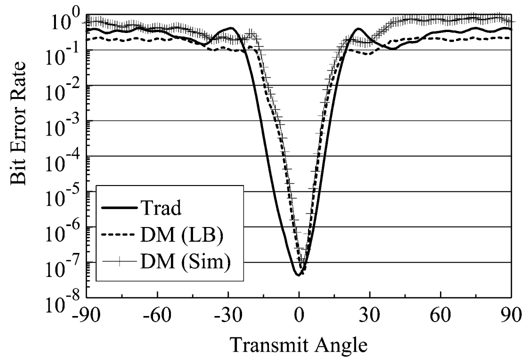


Fig. 8. BER when desired receiver is at broadside for the traditional array (Trad.), the DM array lower bound (LB), and DM simulated BER (Sim).

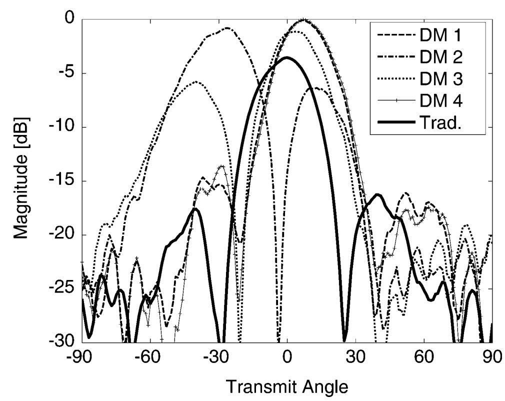


Fig. 9. Normalized radiation patterns when phased to give low BER toward broadside and high BER everywhere else. DM 1 through DM 4 are the radiation patterns when the four different DM constellation points are sent. Also shown is the relative magnitude of the radiation pattern of the traditional array (all elements in-phase) to achieve the same BER toward broadside.

### B. Secure Communication to Broadside

DM can achieve a low BER in a narrow beamwidth toward a desired receiver and still enforce a high BER in other directions. The GA was used to find phase shifts that give a low BER in a $10^\circ$ beamwidth around broadside and a high BER to all other angles in the half-plane from $-90^\circ$ to $+90^\circ$. The resulting BERs given by the lower bound in (11) and by simulation are shown in Fig. 8. In simulations, up to 200 million random bits were transmitted per angle ($1^\circ$ increments) and white Gaussian noise was added to the signal. There is good agreement with the theoretical lower bound and simulation.

Also shown in Fig. 8 is the BER from a traditional array transmitter phased to broadside. This BER is a function of amplitude of the radiation pattern. The expression for the probability of bit error for a traditional QPSK modulation is given by [22]

$$P_b(\text{error}) = Q\left(\sqrt{\frac{E_b}{N_0/2}}\right). \tag{12}$$

The energy per bit in QPSK, $E_b$, is equal to half the symbol energy, $E_s$. $E_s$ is found by taking the square magnitude of the radiation pattern in the direction of interest. The largest magnitude radiation pattern at broadside is produced by the traditional transmitter when all four elements are in phase. This creates a much lower BER at broadside for the traditional array than for the DM array. In order to fairly compare the BER levels in the sidelobe regions, the power of the traditional array was reduced until the BER was the same at broadside as the DM array, while the noise power is kept the same for both transmitters. This means that the traditional array achieves the same low BER toward the desired receiver as the DM array, without spending more power than necessary, which would increase sidelobe power as well as mainlobe power. In this manner, the security in the undesired directions can be compared while the arrays have the same performance in the desired direction. The broadside radiation pattern of the traditional transmitter is shown in Fig. 9, along with radiation patterns created by the four sets of phases of the DM transmitter.

The traditional array and the DM array have the same order of magnitude of BER in the directions away from broadside, but the DM array has a narrower beamwidth in which the BER becomes very low. Thus, at some angles such as $\pm 10^\circ$, the BER of the DM array is several orders of magnitude higher than the BER of the traditional transmitter. While a uniformly fed array has the narrowest possible pattern beamwidth, the DM transmitter has a narrower BER beamwidth due to the fact that it has more freedom to alter constellations.

This extra degree of freedom in altering constellation phase is evident when comparing received constellations at $-50^\circ$. Both arrays achieve about the same high BER (0.2) in this direction. But the signal magnitude of the traditional array in this direction is clearly lower than several of the DM constellation point magnitudes by as much as 13 dB, as can be seen in Fig. 9. Yet, even with this larger signal power, the DM array still manages to keep the BER high. The reason for this can be seen from Fig. 10. The two DM points that have large magnitudes also are very close together in phase, while the other two points have very small magnitudes. Thus, it is difficult for a receiver to distinguish between either pair of points in the presence of noise. The traditional array is able to achieve a low signal magnitude in this direction, but the constellation is still separated as much as possible given that amplitude, providing an opportunity for undesired eavesdropping.

### C. Secure Communication to $-45^\circ$

DM also has advantages over a traditional array when steered away from broadside. Fig. 11 shows the radiation patterns for both transmitters when the desired receiver is at $-45^\circ$ from broadside. The traditional array faces the effects of broadening of the mainlobe and higher sidelobe levels when it is steered away from broadside.

These effects manifest themselves in the BER of the traditional transmitter, shown in Fig. 12. Compared to the DM array, the traditional array has a wider BER beamwidth around the desired direction and the sidelobes cause regions of lower BER in undesired directions. The DM BER has the same narrow beamwidth over which lower BER is transmitted as in Fig. 8.

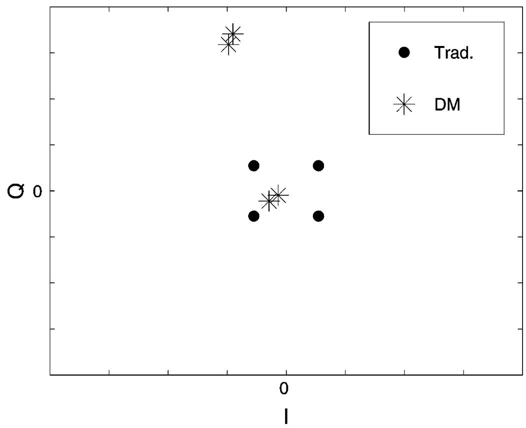


Fig. 10. Constellation diagrams at $-50^\circ$ from broadside for the traditional array and the DM array. While the magnitude of the traditional array's constellation is decreased, it is still able to be decoded, while the DM constellation is, in essence, scrambled.

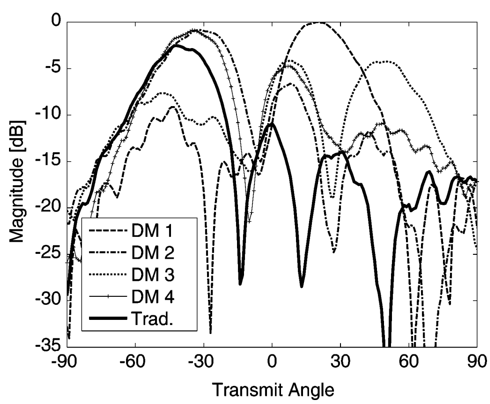


Fig. 11. Normalized radiation patterns when phased to give low BER toward $-45^\circ$ and high BER everywhere else. DM 1 through DM 4 are the resulting radiation patterns when the four different DM constellation points are sent. Also shown is the relative magnitude of the radiation pattern of the traditional array (phased to $-45^\circ$) to achieve the same BER toward $-45^\circ$.

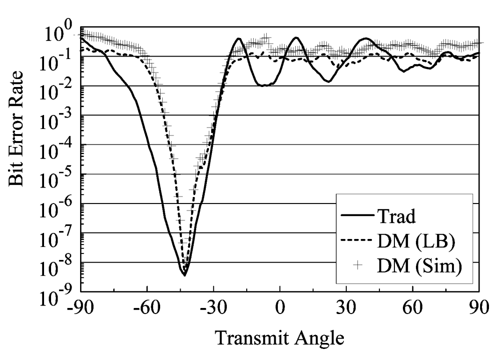


Fig. 12. BER when desired receiver is at $-45^\circ$ shown for traditional array (Trad.), the lower bound of the DM array (LB) and DM simulated BER (Sim).

It also smoothes out sidelobes, displaying a relatively constant high BER in the undesired transmission directions.

## VI. Conclusion

A DM technique has been demonstrated using arrays with driven elements. Unlike previous work similar to DM that used parasitic arrays, using driven elements only requires measurements or simulations for each of the active element patterns instead of every single combination of switch states. Thus, the number of measurements increases linearly with the size of an array instead of exponentially. After these element patterns are known, an efficient GA was shown to either find the phases for transmitting in multiple directions simultaneously or to distort a constellation in all directions except that of the desired receiver. The DM array had a narrower BER beamwidth compared to a traditional array when both were steered toward broadside. Unlike the traditional array, the DM array's BER beamwidth did not broaden when it was steered away from broadside. The directional manipulation of constellation points is possible with DM because the modulation is created at the antenna element level. This is in contrast to a traditional phased array in which the modulation is created at baseband and the same copy sent on each antenna element.

Future work includes the design of reconfigurable antenna elements that can replace the phase shifters in a DM array. Other work includes the study of the transient effects of switching on the digital signal and the inclusion of the crosspolar fields as part of the DM.

## References

[1] W. Kummer, A. Villenueve, T. Fong, and F. Terrio, "Ultra-low sidelobes from time-modulated arrays," *IEEE Trans. Antennas Propag.*, vol. 11, pp. 633–639, 1963.

[2] B. L. Lewis and J. B. Evans, "A new technique for reducing radar response to signals entering antenna sidelobes," *IEEE Trans. Antennas Propag.*, vol. 31, pp. 993–996, 1983.

[3] S. Yang, Y. B. Gan, and P. K. Tan, "Linear antenna arrays with bidirectional phase center motion," *IEEE Trans. Antennas Propag.*, vol. 53, pp. 1829–1835, May 2005.

[4] S. Yang, Y. B. Gan, and P. K. Tan, "A new technique for power-pattern synthesis in time-modulated linear arrays," *IEEE Antennas Wireless Propag. Lett.*, vol. 53, pp. 285–287, 2003.

[5] S. Yang, Y. B. Gan, A. Qing, and P. K. Tan, "Design of a uniform amplitude time modulated linear array with optimized time sequences," *IEEE Trans. Antennas Propag.*, vol. 53, pp. 2337–2339, Jul. 2005.

[6] S. D. Keller, W. D. Palmer, and W. T. Joines, "Electromagnetic modeling and simulation of a directly-modulated L-band microstrip patch antenna," in *Proc. Int. Symp. on Antennas and Propag.*, Jun. 2007, pp. 4489–4492.

[7] E. Baghdady, "Directional signal modulation by means of switched spaced antennas," *IEEE Trans. Commun.*, vol. 38, pp. 399–403, Apr. 1990.

[8] C. M. Elam and D. A. Leavy, "Secure communication using array transmitter," U. S. Patent 6 275 679, Aug. 14, 2001.

[9] A. Babakhani, D. B. Rutledge, and A. Hajimiri, "A near-field modulation technique using antenna reflector switching," in *Proc. IEEE Int. Solid State Circuits Conf.*, Feb. 2008, pp. 188–189.

[10] A. Babakhani, D. B. Rutledge, and A. Hajimiri, "Transmitter architectures based on near-field direct antenna modulation," *IEEE J. Solid-State Circuits*, vol. 43, no. 12, pp. 2674–2692, Dec. 2008.

[11] R. L. Haupt and R. A. Shore, "Experimental partially adaptive nulling in a low sidelobe phased array," in *Proc. IEEE Antennas Propag. Soc. Int. Symp.*, 1984, pp. 823–826.

[12] R. L. Haupt, "Phase-only adaptive nulling with a genetic algorithm," *IEEE Trans. Antennas Propag.*, vol. 45, pp. 1009–1015, Jun. 1997.

[13] R. J. Mailloux, *Electronically Scanned Arrays*, 1st ed. San Rafael, CA: Morgan & Claypool, 2007.

[14] D. M. Pozar, "The active element pattern," *IEEE Trans. Antennas Propag.*, vol. 42, pp. 1176–1178, Aug. 1994.

[15] R. C. Hansen, "Comments on 'The active element pattern'," *IEEE Trans. Antennas Propag.*, vol. 43, pp. 634–638, Jun. 1995.

[16] R. L. Haupt, "Thinned arrays using genetic algorithms," *IEEE Trans. Antennas Propag.*, vol. 42, pp. 993–999, Jun. 1994.

[17] K. K. Yan and Y. Lu, "Sidelobe reduction in array-pattern synthesis using genetic algorithm," *IEEE Trans. Antennas Propag.*, vol. 45, pp. 1117–1122, Jun. 1997.

[18] J. W. Craig, "A new, simple and exact result for calculating the probability of error for two-dimensional signal constellations," in *Proc. IEEE MILCOM'91*, 1991, pp. 571–575.

[19] L. Szczecinski, C. Gonzalez, and S. Aissa, "Exact expression for the BER of rectangular QAM with arbitrary constellation mapping," *IEEE Trans. Commun.*, vol. 54, pp. 389–392, Mar. 2006.

[20] L. Szczecinski, S. Aissa, C. Gonzalez, and M. Bacic, "Exact evaluation of BER for arbitrary modulation and signaling in AWGN channel," in *Proc. IEEE GLOBECOM*, 2005, pp. 1234–1238.

[21] A. Goldsmith, *Wireless Communications*, 1st ed. New York, NY: Cambridge Univ. Press, 2005.

[22] J. G. Proakis, *Digital Communications*, 4th ed. Boston, MA: McGraw-Hill, 2001.


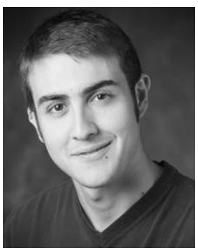

**Michael P. Daly** (SM'09) was born in San Juan, Puerto Rico, on October 31, 1984. He received the B.S. degree (with highest honors) and M.S. degree in electrical engineering from the University of Illinois at Urbana-Champaign, in 2007 and 2008, respectively, where he is currently working toward the Ph.D. degree.

His research interests include reconfigurable antennas, arrays, and digital communications.

Mr. Daly is the recipient of an NDSEG fellowship.

**Jennifer T. Bernhard** (S'89–M'95–SM'01) was born on May 1, 1966, in New Hartford, NY. She received the B.S.E.E. degree from Cornell University in 1988 and the M.S. and Ph.D. degrees in electrical engineering from Duke University, Durham, NC, in 1990 and 1994, respectively, with support from a National Science Foundation Graduate Fellowship.

While at Cornell, she was a McMullen Dean's Scholar and participated in the Engineering Co-op Program, working at IBM Federal Systems Division in Owego, New York. During the 1994–95 academic year she held the position of Postdoctoral Research Associate with the Departments of Radiation Oncology and Electrical Engineering, Duke University, where she developed RF and microwave circuitry for simultaneous hyperthermia (treatment of cancer with microwaves) and MRI (magnetic resonance imaging) thermometry. From 1995 to 1999, she was an Assistant Professor in the Department of Electrical and Computer Engineering, University of New Hampshire, where she held the Class of 1944 Professorship. Since 1999, she has been with the Electromagnetics Laboratory, Department of Electrical and Computer Engineering, University of Illinois at Urbana-Champaign, where she is now a Professor. In 1999 and 2000, she was an NASA-ASEE Summer Faculty Fellow at the NASA Glenn Research Center in Cleveland, OH. Her research interests include reconfigurable and wideband microwave antennas and circuits, wireless sensors and sensor networks, high speed wireless data communication, electromagnetic compatibility, and electromagnetics for industrial, agricultural, and medical applications, and has two patents on technology in these areas. Her industrial experience includes work as a Research Engineer with Avnet Development Labs and, more recently, as a private consultant for members of the wireless communication and sensors community.

Prof. Bernhard received the NSF CAREER Award in 2000. She is also an Illinois College of Engineering Willett Faculty Scholar and a Research Professor in Illinois' Micro and Nanotechnology Laboratory, the Coordinated Science Laboratory, and the Information Trust Institute. She and her students received the 2004 H. A. Wheeler Applications Prize Paper Award from the IEEE Antenna and Propagation Society for their paper published in the March 2003 issue of the IEEE TRANSACTIONS ON ANTENNAS AND PROPAGATION. She served as an Associate Editor for IEEE TRANSACTIONS ON ANTENNAS AND PROPAGATION from 2001 to 2007 and served as an Associate Editor for IEEE ANTENNAS AND WIRELESS PROPAGATION LETTERS from 2001 to 2005. She is also a member of the editorial board of *Smart Structures and Systems*. She is a member of URSI Commissions B and D, Tau Beta Pi, Eta Kappa Nu, Sigma Xi, and ASEE. She is a Senior Member of the IEEE and served as an elected member of the IEEE Antennas and Propagation Society's Administrative Committee from 2004 to 2006. She was President Elect and President of the IEEE Antennas and Propagation Society in 2007 and 2008, respectively. At Duke, she was also an organizing member of the Women in Science and Engineering (WISE) Project, a graduate student-run organization designed to improve the climate for graduate women in engineering and the sciences.